

Elasto-buoyant heavy spheres: a unique way to test non-linear elasticity

Aditi Chakrabarti and Manoj K. Chaudhury

Department of Chemical Engineering, Lehigh University, Bethlehem, Pennsylvania 1801S, United States

Serge Mora*

Laboratoire de Mécanique et de Génie Civil. UMR 5508,

Université Montpellier and CNRS. 163 Rue Auguste Broussonnet. F-34090 Montpellier, France.

Yves Pomeau

University of Arizona, Department of Mathematics, Tucson, USA.

(Dated: April 8, 2022)

Extra-large deformations produced by a heavy bead gently deposited on the horizontal surface of an incompressible ultra-soft elastic medium are investigated, providing a basis for a better understanding of highly strained elastic materials. These experiments stipulate a scaling law for the penetration depth of the bead inside the gel, $\delta \sim a^{3/2}$, a being the radius of the bead, which is in quantitative agreement with an original asymptotic analytic model developed in this article. This model highlights the role of buoyancy and the effects of the strong non-linearities coming from the large deformations.

PACS numbers: 46.25.-y, 83.85.Cg, 46.05.+b, 83.80.Va

Soft solids undergoing large deformations exhibit fascinating and puzzling mechanical behaviours. Some complex patterns observed in biology [1–3], in geological processes [4], or with synthetic materials [5–10] are the consequence of mechanical instabilities or of weak forces [11–19], involving finite deformations of solid bodies. Large elastic deformations are also crucial in emerging techniques, for instance computer-assisted surgery. In computer-aided surgical simulations [20–22], the software aims to predict, before an incision or a suture is made, the ensuing displacement and the deformations of the surrounding organs. Numerical methods make all these possible, even with complex environments, provided that the deformations remain infinitesimal [23, 24]. The problem is much more difficult with finite deformations, current methods of calculation being far from being well established [25] in many of these cases. This limitation is to be overcome since many tissues commonly undergo large deformations, either in their natural environment or during surgery.

Here we explore such large deformations of soft elastic gels by looking at a model problem, namely the changes due to the weight of a steel bead gently deposited on the horizontal flat surface of a gel. The compliant gel is deformed by the load exerted by the heavy bead as it sinks slowly. The bead becomes elasto-buoyant once the forces applied by the elastic gel on the bead counterbalance its weight. The penetration depth of the bead in the gel below the initially flat surface, δ , is measured for several values of the shear modulus of the gel and of the radius a of the bead. When the elastic modulus is sufficiently small and the sphere radius large, δ is larger than a , the bead is totally engulfed inside the elastic gel (Fig.1-b). In this regime δ is found to scale as $a^{3/2}$. An asymptotic analysis sketched in the second part of the paper illustrates that this exponent of a is incompatible with an ideal neo-Hookean model that leads to a divergence of elastic deformation energy. Its manifestation becomes uniquely evident by studying

the convergence criterion of an extended non-Hookean model.

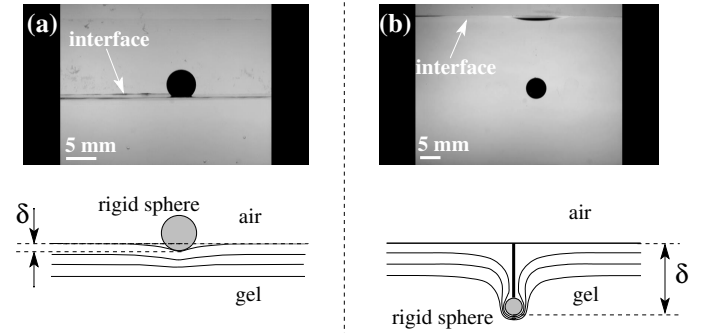


FIG. 1: **(Top)** Side views of two transparent cells filled with a polyacrylamide gel having a shear modulus of 160 Pa (a) and 13 Pa (b). Two identical steel beads (5 mm diameter) have been deposited in the free air-gel interface. The vertical downshifts are respectively $\delta = 0.03 \delta_0$ and $\delta = 320 \delta_0$.

(Bottom) Schematic of the experiments. The bold line draws the air-gel interface.

Physically cross-linked polyacrylamide gels are used in the experiments reported below. Gels of shear moduli ranging from 13 Pa to 2930 Pa are prepared from solutions of various concentrations (2.9% - 6.4%) of monomers [N-(hydroxymethyl)-acrylamide (48% solution in deionized water, Sigma Aldrich)]. The desired aqueous solution of the monomer is first purged with ultra-pure nitrogen gas for 30 minutes. Following this step, the catalyst (potassium persulfate, 0.25 wt%, Sigma Aldrich) is well stirred in the solution. On addition of the initiator [N,N,N,N-tetramethylethylenediamine (TEMED), 0.3 wt%, Sigma Aldrich], the polymerization reaction is triggered. The gel

solutions is cured in home-built glass containers (70 mm x 50 mm x 40 mm), the inner walls of which are grafted with a thin layer (~ 5 nm) of polydimethyl siloxane chains (DMS T-22, Gelest Inc.) so that the gel solution contacted the walls at 90° to ensure that the surface of the cured gel is flat. All the experiments are performed after 2 hours of gelation. In order to measure precisely the shear modulus μ of the gel, a thin gel slab (50mm x 25mm x 1mm) with exactly the same composition of the previous gel is cured between two parallel glass plates. They undergo small-strain shear deformation laterally and the shear modulus of the gel is found from the resonant mode of vibration, $\mu = 4\pi^2\omega^2 mH/A$ where ω is the resonant frequency, m is the mass on the gel slab, H its thickness and A its area of contact with the upper glass substrate. We use high speed imaging (Redlake MotionPro) to obtain the resonant frequency of vibration of the thin gel slabs. More details on the experimental procedure for the estimation of the shear moduli can be found in [26].

Steel spheres (density 7.8 g/cc, E52100 Alloy Steel, McMaster Carr) are sonicated in acetone for 10 minutes and dried with a stream of pure nitrogen. Each steel sphere (diameters 1 - 10 mm) is gently placed on the gel surface, one by one, starting from the smallest size, and its side-view image is captured by a CCD camera (MTI 72). Dissipative processes within the gel dampen any oscillations, and the spheres sink until they become stagnant in the polyacrylamide gel. The depth of submersion, δ , is measured from the upper surface of the gel till the base of sphere, that denoting the net downward displacement due to the inclusion of the spherical particle on the surface (Fig.1). The cells are large enough to avoid any wall effect: the penetration depths of the beads do not change with the size of the cells. If the bead is too small and the gel is too stiff, the surface bends slightly under the weight of the bead and $\delta \ll a$ (Fig.1-a). Increasing the bead radius or decreasing the elastic modulus, the particle starts to submerge itself to a considerable depth inside the gel. The surface of the gel wraps around the particle and closes to create a line singularity connecting the particle to the free surface of the gel (Fig.1-b). Strings of tiny air bubbles appear in this thin channel, which soon coalesce and escape through it while the channel further closes due to the auto-wetting forces of the gel's surface. If the surface of the gel is premarked with ink spots, it is easy to visualize that the surface of the gel becomes appreciably stretched while the sphere sinks through the gel while still connected to the free surface via a thin channel. It is also possible to release ink inside the gel in the form of thin vertical lines with the help of a fine needle, which bend toward the sphere in a dramatic way when the sphere is released inside the gel. A substantial amount of tensile strain is thus developed in the gel network parallel to the free surface that penetrates to a significant depth inside the gel. This was reported in a previous article [9], but without a detailed analysis.

The reversibility of these deformations is tested with the softest gel, whose shear modulus is 13 Pa. By varying only the system temperature, the elastic modulus of polyacrylamide gels changes. A thin layer of Paraffin oil is poured over the

μ (Pa)	2930	1560	1160	540	140	110	101	56	25	13
$\alpha (\pm 0.15)$	1.8	2.0	1.94	1.72	1.52	1.51	1.87	1.66	1.52	1.42
k	0.72	1.17	1.00	0.80	1.04	1.12	0.95	0.94	1.10	1.52

TABLE I: First line: measured shear modulus. Second line: exponent α obtained by fitting a power law function $\delta \sim a^\alpha$ with the experimentally measured downshift δ as a function of the bead radius a . Third line: dimensionless prefactor k (see the text).

gel to avoid its surface from drying. The temperature of the gel is monitored by placing a thermometer inside an identical sample of gel in a similar sized container, placed inside the oven. After the gel is heated to 70°C , a 5 mm diameter steel sphere is released into it through the layer of paraffin oil. The depth of the sphere is measured at this temperature while it is in the oven. As the gel is gradually cooled, the sphere sinks deeper inside it. We wait for an hour between acquiring data for the depth of sphere at each temperature to allow the gel to equilibrate reasonably well. After the gel is cooled to about 5°C , it is heated again that decreases the depth of the embedded steel sphere (Heating Cycle, inset of Fig.2). The depth of submersion of the sphere plotted as a function of the temperature for both the cooling and the heating cycles (inset of Fig.2) shows that there is a little hysteresis in this system, in that the difference in the depths of the sphere for a given temperature is within 5%. We conclude that the deformations of the gel generated by a bead are predominantly reversible.

The measured penetration depth, δ , is plotted versus the normalized radius $\frac{a}{\delta_0}$ of the steel spheres in log-scales in Fig.2, for the different gels (13 Pa - 2930 Pa) and different radii. δ_0 is a material length-scale $\delta_0 = \frac{\mu}{\Delta\rho g}$, where μ is the shear modulus of the gel, $\Delta\rho$ is the difference in the densities of steel and the gel, and g is the gravitational acceleration. The reason why we use $\Delta\rho$ instead of the density of steel will appear below. For a given gel composition we fit the data with the power law function $(\delta/\delta_0) = k(a/\delta_0)^\alpha$ with adjustable parameters, α and k . Different values of these parameters are found from one gel to another (see Tab. I).

The values of the exponent α lie between 1.5 and 2, depending on the gel (Tab. I). $\alpha \simeq 2$ for the gels with the higher shear moduli for which $\delta < a$ for all the tested beads (the beads are not engulfed), and $\alpha \simeq 1.5$ for the softest gels for which $\delta > a$ for all the tested beads (the beads are totally engulfed). It would be presumptuous to infer, from these data, a tendency for the changes in the prefactor, k , with the variations of the shear modulus. We just conclude here that k is always of order one, and does not vary dramatically from one gel to another.

We now focus on the large deformations and theoretically derive a scaling law for δ by considering the balance of the vertical forces and assuming $\delta \gg a$. In the opposite limit, $\delta \ll a$, the deformations are infinitesimal and this classical problem of indentation can be treated within the JKR theory [27, 28].

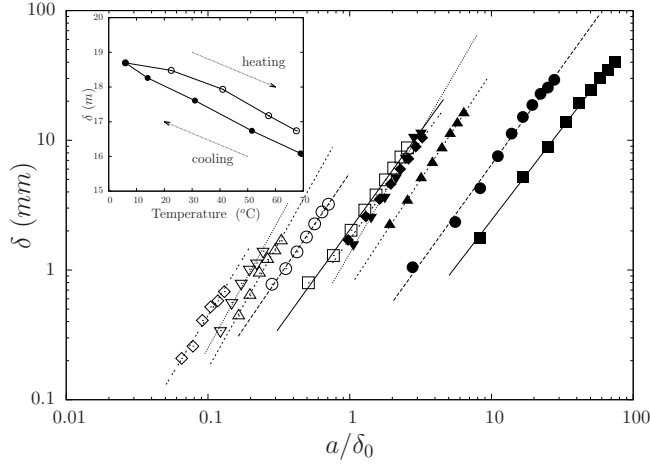


FIG. 2: Plot of the penetration depth of a sphere (δ) as a function of its dimensionless radius a/δ_0 , for various shear modulus of the gel (■ : 13 Pa ; ● : 25 Pa ; ▲ : 56 Pa ; ▼ : 101 Pa ; ◆ : 110 Pa ; □ : 140 Pa ; ○ : 540 Pa ; △ : 1160 Pa ; ▽ : 1560 Pa ; ◇ : 2930 Pa). Lines are for the best fits via scaling law functions $\delta = k\delta_0(a/\delta_0)^\alpha$ (see Tab. I). Inset: Depth of submersion of a 5 mm diameter steel sphere in a soft gel varying as a function of its temperature. The experiments in the cooling cycle was performed first following which the gel was heated systematically to obtain the data for the heating cycle.

The axis of symmetry being the vertical axis, the two coordinates changed by the deformation are the radius in the horizontal plane, r , and the vertical coordinate, z . The deformation maps the undisturbed state with coordinates (r, z) to a disturbed state $(R(r, z), Z(r, z))$, or, in radial coordinates from coordinates $(\tilde{r}; \theta)$ to $(R(\tilde{r}, \theta); Z(\tilde{r}, \theta))$ with \tilde{r} radius and θ polar angle of the $(r; z)$ plane. In this Lagrangian framework, an actual location in space is parametrized by the coordinates of its preimage in the undisturbed (rest) state (see Fig.3). Assuming $a \ll \delta$, the unique relevant length-scale for the displacements is δ . Therefore the most general expressions for the coordinates in the deformed configuration are

$$R = \delta \cdot f\left(\frac{r}{\delta}, \frac{z}{\delta}\right), \quad (1)$$

$$Z = \delta \cdot g\left(\frac{r}{\delta}, \frac{z}{\delta}\right), \quad (2)$$

f and g being two numerical functions whose expressions only depends on the constitutive law of the elastic medium.

For an incompressible and isotropic elastic material, the elastic energy density \mathcal{W} is a function of the first and the second invariants of the left-Cauchy-Green deformation tensor $C = FF^T$, F being the deformation gradient. In cylindrical coordinates with an azimuthal invariance these invariants reads $I_1 = R_{,r}^2 + \frac{R_{,z}^2}{r^2} + R_{,z}^2 + Z_{,r}^2 + Z_{,z}^2$ and $I_2 = (R_{,r}^2 + Z_{,z}^2)^2 + (R_{,z}^2 + Z_{,r}^2)^2 + 2(R_{,r}R_{,z} + Z_{,z}Z_{,r})^2 + \frac{R^4}{r^4}$, where indices preceded by a comma denote respective partial derivatives. With the neo-Hookean model, a fair representa-

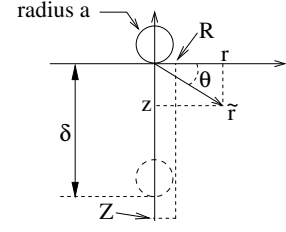


FIG. 3: Sketch of the system in the rest state (solid lines), with the bead at the surface. A point of the gel in the rest state is located with coordinates (r, z) . \tilde{r} is the distance from the initial contact point of the bead. In the deformed state, the point that was at (r, z) is located at $R(r, z), Z(r, z)$ and the vertical displacement of the bead is $Z(0, 0) = \delta$.

tion of many soft gels for strains up to several hundred percent, $\mathcal{W} = \frac{\mu}{2}I_1$. Note that beyond a certain deformation, the neo-Hookean model necessarily fails: elasticity of rubber-like materials originates from unfolding polymer chains. Once these chains reach their full extension, the energy cost for a supplementary unfolding diverges so that a further deformation is accompanied by a diverging additional elastic energy, in contrast with the ideal neo-Hookean law. In what follows, we do not restrict ourselves to the neo-Hookean case.

The elastic energy of the system reads:

$$\mathcal{E}_{el} = 2\pi \int dz \int dr r \mathcal{W}(I_1, I_2). \quad (3)$$

From Eqs. 1 and 2 the invariants I_1 and I_2 are two dimensionless functions depending only on r/δ and z/δ . We first assume that the integral in Eq.3 converges, a non trivial assumption that will be justified below. Within this hypothesis, the elastic energy (Eq.3) is proportional to δ^3 with a coefficient C having the dimension of a shear modulus and depending on the mechanical properties of the elastic solid.

We consider deformations that preserve the volume, as is the case with the elastic gels used in the experiments. Since the sphere is supposed to be totally engulfed with $\delta \gg a$, the surface of the deformed gel is fairly flat and horizontal. A supplementary (virtual) downshift δ' produces an opposite rise of the same volume of gel. Therefore the gravitational energy variation of the system consisting of the sphere plus the gel is $\frac{4}{3}\pi a^3 \Delta \rho g \delta'$ and we conclude that the gravitational energy shift is $\mathcal{E}_{gr} \simeq \frac{4}{3}\pi a^3 \Delta \rho g \delta$ in the limit we are dealing with.

In the equilibrium state the δ -derivatives of \mathcal{E}_{gr} and $\mathcal{E}_{el} = C\delta^3$ are equal, giving the scaling law valid for $\delta \gg a$:

$$\delta \sim a^{3/2} (\Delta \rho g)^{1/2}. \quad (4)$$

This prediction is in quantitative agreement with the experimental observations.

The scaling law (Eq.4) is based on the non-trivial hypothesis of a convergent integral in Eq.3. However, within

the assumption of an unique length-scale, δ , this integral may diverge at the boundary $\tilde{r} = 0$ where the strain is concentrated. This is because even if $a \ll \delta$, the length a is not negligible compared to \tilde{r} near the origin ($\tilde{r} = 0$). A convergent integral ensures that the integral does not depend on a as well as the scaling law Eq.4. On the contrary, a non-convergent integral means that the length a has to be taken into account for the calculation of the energy, and the scaling law Eq.4 would therefore not apply. As shown below, the integral in Eq.3 is convergent, by formally taking $a = 0$, for any real material, and therefore it does not depends on the radius a , in contrast with an ideal neo-Hookean solid.

Using a variational formulation, the total energy reads:

$$\mathcal{E} = \frac{4}{3}\pi\Delta\rho a^3 gZ(0,0) + 2\pi \int dz \int dr (\mathcal{W} - q\mathcal{D}) r, \quad (5)$$

where $q(r, z)$ is a Lagrange multiplier imposing the incompressibility condition $\mathcal{D} \equiv \det(\nabla F) = 1$. In cylindrical coordinates one gets $\mathcal{D} = \frac{R}{r} (R_{,r}Z_{,z} - R_{,z}Z_{,r})$. The first term in Eq.5 is for the potential energy of the bead in the gravity field.

By variation with respect to R and Z , one gets the Cauchy-Poisson equations in cylindrical coordinates:

$$\left(\frac{\partial (\mathcal{W} - q\mathcal{D}) r}{\partial R_{,r}} \right)_{,r} + \left(\frac{\partial (\mathcal{W} - q\mathcal{D}) r}{\partial R_{,z}} \right)_{,z} = \frac{\partial (\mathcal{W} - q\mathcal{D}) r}{\partial R} \quad (6)$$

$$\left(\frac{\partial (\mathcal{W} - q\mathcal{D}) r}{\partial Z_{,r}} \right)_{,r} + \left(\frac{\partial (\mathcal{W} - q\mathcal{D}) r}{\partial Z_{,z}} \right)_{,z} = \frac{4\pi\Delta\rho g a^3}{3} \delta^2(r, z) \quad (7)$$

where $\delta^2(r, z)$ is the 2D Dirac distribution.

Consider a sphere centered at the origin and of radius \tilde{r} much bigger than a (radius of the bead) and much smaller than δ . This defines a short distance with respect to the large scale behaviour of the elastic deformation and a large distance with respect to the size of the sphere. To establish the convergence conditions of the integral providing the elastic energy we assume a power law of the distance \tilde{r} to the origin for the displacements: $Z = \tilde{r}^\beta f_1(\theta)$ and $R = \tilde{r}^\gamma f_2(\theta)$. The gel being vertically stretched and horizontally squeezed in the vicinity of the bead, $\gamma > \beta$. The incompressibility condition yields $\gamma = \frac{3-\beta}{2}$. We first assume that the elastic energy density \mathcal{W} follows itself the power law $\mathcal{W} \propto I_1^{\alpha_1}$.

Denoting $\sigma_{zr} = \frac{\partial(\mathcal{W}-q\mathcal{D})r}{\partial Z_{,r}}$ and $\sigma_{zz} = \frac{\partial(\mathcal{W}-q\mathcal{D})r}{\partial Z_{,z}}$, the left hand side of Eq.7 is the divergence of the z-components of the stress tensor σ . The right hand side being a delta-like charge density, one gets: $\sigma_{zr} \sim 1/\tilde{r}$ and:

$$\frac{\partial (\mathcal{W} - q\mathcal{D}) r}{\partial Z_{,r}} = r \frac{\partial \mathcal{W}}{\partial I_1} \frac{\partial I_1}{\partial Z_{,r}} + qRR_{,z} \sim \frac{1}{\tilde{r}}. \quad (8)$$

Neglecting $qRR_{,z}$ in Eq.8 one obtains after some algebra:

$$\beta = \frac{2\alpha_1 - 3}{2\alpha_1 - 1}. \quad (9)$$

From Eq.6, $q \sim \tilde{r}^{(4\alpha_1-6)/(1-2\alpha_1)}$ and consequently $qRR_{,z} \sim \tilde{r}^{(7-2\alpha_1)/(2\alpha_1-1)}$ which is negligible compared to $r \frac{\partial \mathcal{W}}{\partial I_1} \frac{\partial I_1}{\partial Z_{,r}} \sim 1/\tilde{r}$, showing that the term $qRR_{,z}$ is negligible in Eq.8.

The total elastic energy is therefore $\mathcal{E}_{el.} \sim \int \tilde{r}^2 I_1^{\alpha_1} d\tilde{r} \sim \int \tilde{r}^{2/(1-2\alpha_1)} d\tilde{r}$. This integral is convergent near $\tilde{r} = 0$ for $2/(1-2\alpha_1) > -1$, i.e. $\alpha_1 > 3/2$. This is also the condition for Z to be convergent, i.e. for the displacement of the bead to be finite. Note that since the strain is a derivative of the displacement, it may diverge although the displacement does not.

We conclude that the scaling law Eq.4 applies for $\mathcal{W} \sim I_1^{\alpha_1}$ with $\alpha_1 > 3/2$. For a neo-Hookean solid ($\alpha_1 = 1$) the integral of Eq.3 evaluated by formally taking $a = 0$ diverges and the elastic energy depends on a : the scaling law Eq.4 does not apply.

In the same way, the elastic energy does not depend on a with the density energy function $\mathcal{W} \sim I_1^{\alpha_1} I_2^{\alpha_2}$ for $\alpha_1 + 2\alpha_2 > \frac{3}{2}$.

In the experiments, the plastic limit of the gel is never reached. Due to the finite maximum stretch of the polymer chains constituting the material, the strain energy density function, \mathcal{W} , diverges to infinity beyond a certain strain. This divergence results in a stronger and stronger increase of \mathcal{W} with I_1 , I_2 , or both, which is associated with increasing values of the exponents α_1 and/or α_2 [29, 30]. Starting from low to moderate strains for which the neo-Hookean model applies far from the bead, stiffer energy density functions are encountered next to the bead to prevent infinite strains. Therefore, any real material satisfies the criteria for the elastic energy to scale as δ^3 in an area surrounding the beads. This explains our experimental observation, i.e. $\delta \sim a^{3/2}$ for $a \ll \delta$.

We have demonstrated that the downshift δ of a heavy bead of radius a deposited on the horizontal surface of an incompressible elastic gel follows the scaling law $\delta \sim a^{3/2}$ provided that $a \ll \delta$. This scaling results from the balance between the elastic energy and the gravitational energy. It is based on the strain-stress relationship at large deformations. The exponent $3/2$ for the radius is independent of this strain-stress relation provided that the increase in the elastic energy density (\mathcal{W}) with the strain is stiff enough. On the contrary, the prefactor in the scaling law necessarily depends on this relationship. Indentation experiments could be a way to assess some characteristics of elastic materials under large strains, as strain hardening properties. For instance, the elastic energy has been found to be proportional to δ^3 : $\mathcal{E}_{el} = C\delta^3$. The constant C contains information on the gel behavior at large deformations. Balancing the δ -derivatives of the energies and keeping the prefactors yields $\frac{\delta}{\delta_0} = \sqrt{\frac{4\pi\mu}{9C}} \left(\frac{a}{\delta_0} \right)^{3/2}$. The square root is the prefactor k in table I, giving a way to calculate C .

We have focused on the limit $\delta \gg a$. Intermediate regimes are also of interest and should be studied in the future, such

as partially engulfed beads with finite deformations, or fully engulfed beads with a similar to δ .

* serge.mora@umontpellier.fr

- [1] M. B. Amar and P. Ciarletta, *Journal of the Mechanics and Physics of Solids* **58**, 935 (2010).
- [2] E. Hohlfeld and L. Mahadevan, *Physical Review Letters* **109**, 025701 (2012).
- [3] J. Dervaux and M. B. Amar, *Annual Review of Condensed Matter Physics* **3**, 311 (2012).
- [4] M. Biot, *Appl. Sci. Res.* **12**, 168 (1963).
- [5] J. Kim, J. Yoon, and R. Hayward, *Nature Mater.* **9**, 159 (2010).
- [6] J. Biggins, B. Saintyves, Z. Wei, E. Bouchaud, and L. Mahadevan, *Proceedings of the National Academy of Sciences* **110**, 12545 (2013).
- [7] T. Tallinen, J. Biggins, and L. Mahadevan, *Phys. Rev. Lett.* **110**, 024302 (2013).
- [8] B. Saintyves, O. Dauchot, and E. Bouchaud, *Phys. Rev. Lett.* **111**, 047801 (2013).
- [9] A. Chakrabarti and M. Chaudhury, *Langmuir* **29**, 6926 (2013).
- [10] S. Mora, T. Phou, J. M. Fromental, and Y. Pomeau, *Phys. Rev. Lett.* **113**, 178301 (2014).
- [11] C. Y. Hui, A. Jagota, Y. Y. Lin, and E. J. Kramer, *Langmuir* **18**, 1394 (2002).
- [12] M. Adda-Bedia and L. Mahadevan, *Proceedings of the Royal Society* **462**, 3233 (2006).
- [13] S. Mora, T. Phou, J. M. Fromental, L. M. Pismen, and Y. Pomeau, *Phys. Rev. Lett.* **105**, 214301 (2010).
- [14] S. Mora, M. Abkarian, H. Tabuteau, and Y. Pomeau, *Soft Matter* **7**, 10612 (2011).
- [15] N. Nadermann, C. Hui, and A. Jagota, *PNAS* **110**, 10541 (2013).
- [16] R. Style, C. Hyland, R. Boltyanskiy, J. Wettlaufer, and E. Dufresne, *Nature Communications* **4**, 2728 (2013).
- [17] R. Style, Y. Che, R. Boltyanskiy, J. Wettlaufer, L. Wilen, and E. Dufresne, *Phys. Rev. Lett.* **110**, 066103 (2013).
- [18] S. Mora, C. Maurini, T. Phou, J. M. Fromental, B. Audoly, and Y. Pomeau, *Phys. Rev. Lett.* **111**, 114301 (2013).
- [19] D. Paretkar, X. Xu, C. Hui, and A. Jagota, *Soft Matter* **10**, 4084 (2014).
- [20] A. Liu, F. Tendick, K. Cleary, and C. Kaufmann, *Presence-Teleoperators and Virtual Environments* **12**, 599 (2004).
- [21] N. Seymour, A. Gallagher, S. Roman, M. O'Brien, V. Bansal, D. Andersen, and R. Satava, *Annals of Surgery* **236**, 458 (2002).
- [22] L. Sturm, J. Windsor, P. Cosman, P. Cregan, P. Hewett, and G. Maddern, *Annals of Surgery* **248**, 166 (2008).
- [23] S. Cotin, H. Delingette, and N. Ayache, *IEEE trans. on Visualization and Computer Graphics* **5**, 62 (1999).
- [24] Z. Taylor, M. Cheng, and S. Ourselin, *IEEE Transactions on Medical Imaging* **27**, 650 (2008).
- [25] S. Misra, K. Ramesh, and A. Okamura, *Presence-Teleoperators and Virtual Environments* **17**, 463 (2008).
- [26] A. Chakrabarti and M. Chaudhury, *Langmuir* **30**, 4684 (2014).
- [27] H. Hertz, *J. für reine und angewandte Mathematik* **92**, 156 (1881).
- [28] K. Johnson, K. Kendall, and A. Roberts, *Proc. R. Soc. Lond. Ser. A.* **324**, 301 (1971).
- [29] R. Ogden, *Non-Linear Elastic Deformations* (Ellis Horwood Limited, Chichester, 1984).
- [30] A. Gent, *International Journal of Non-Linear Mechanics* **40**, 165 (2005).